NOVEL BISTABLE HAMMER VALVE FOR DIGITAL HYDRAULICS

Jukka-Pekka Uusitalo[1], Ville Ahola[2], Lasse Soederlund[1], Matti Linjama[2], Maarit Juhola[1] and Lauri Kettunen[1]

[1]*Department of Electronics, Electromagnetics, Tampere University of Technology,*
[2]*Department of Intelligent Hydraulics and Automation, Tampere University of Technology*
Korkeakoulunkatu 3, 33720 Tampere, Finland
E-mail: jukka-pekka.uusitalo@tut.fi

ABSTRACT

This paper presents a fast and small on/off actuator – called the bistable hammer actuator – which requires only a small amount of work to switch between two stable positions. This actuator is combined with a suitable hydraulic part. The combination – called the hammer valve – is analyzed with multiphysical models including dynamic electromagnetic and static fluid mechanic models. A prototype is built and measured to verify the analysis. Smaller and faster valves are critical in digital hydraulics, and the results show the presented valve is competitive for the needs of digital hydraulics.

Keywords: bistable on/off valve, small valve, fast valve, permanent magnet

1 Introduction

Digital hydraulics means hydraulic control implemented with parallel on/off valves. A single valve is thus a critical part of a digital hydraulic control system, and smaller and faster valves are needed to make digital hydraulics competitive (Linjama, 2003; Linjama, 2007; Linjama, 2008).

A typical valve in digital hydraulics is a directly driven on/off seat valve including a solenoid and a spring as the actuator for bidirectional movement. In the literature ideas to reduce solenoid valve's switching time and volume with help of a bistable construction or add on electronics have been presented in Kajima (1995) and Kallenbach (1999). In the Sturman digital latching spool valve presented in Johnson (2001) and in the bistable valve presented in Uusitalo (2009), electromagnetic and hydraulic parts are designed together and integrated. The Sturman valve is a spool valve that exploits boosting while the valves designed in Uusitalo (2009) and in this paper are seat valves studied without extra electronics (e.g. boosting with a booster circuit or cooling with a fan).

To characterize valves we introduce a so called flow density number which is one of our key properties in valves. It is defined as the flow capacity divided by the volume of the valve. In our knowledge, the bistable seat valve presented in Uusitalo (2009) has the highest flow density values and the shortest response time among all directly driven on/off valves and especially seat valves. This valve is a an integrated combination of an electromagnetic actuator that exploits permanent magnets and a non-leaking seat type hydraulic part with reduced opening forces (Lauttamus, 2006).

In hydraulics, the bistability of the device depends often on the flow rate. Another bistable hydraulic seat part is presented in Karvonen (2009). A microhinge (Tsay, 2004) and an elastic beam (Garstenauer, 1999) are examples of mechanical bistability.

This paper presents a valve where the bistable actuator presented in Uusitalo (2009) is replaced by a novel actuator while the hydraulic part is essentially the same. The new actuator is referred to as the bistable hammer actuator. Previously much the same bistable actuators have been presented for example in Burmeister (1967) and Lesquesne (1990), but without the hammer actuation.

2 Behavior of Hammer Actuator

The word hammer usually refers to a situation, where an accelerated part with kinetic energy is colliding with a target part. The speed of the accelerating part is often

This manuscript was received on 16 July 2010 and was accepted after revision for publication on 8 October 2010

slowly accelerated whereas the collision and the transform of the kinetic energy to heat, work or kinetic energy of the target part are more sudden events. The key factor in a collision process is that it enables a high transient force. For example, in case of a human, hammer, nail, and wood the nail needs a high transient force to split its way in the wood.

In case of the hammer valve, there is also an accelerating part and a target part. The target part is connected to a hydraulic armature. When the accelerating part has gained speed it hits the target part and a high impulse force is exerted on it. If the force during the impulse is high enough, a certain hydraulic threshold force is exceeded and the valve opens to at least ajar. Then, if the hydraulic forces drop fast enough, the kinetic energy of the moving parts suffice to open the valve.

Of the known hydraulic parts, a seat part with several restrictions presented in Lauttamus (2006) suits well with the hammer actuator. It has a rapidly decreasing force at the opening and the hydraulic force has a bistable form.

The bistable hammer actuator has similar usability properties as the bistable actuator presented in Uusitalo (2009). That is for example, the valve can be driven transiently at overfrequencies, meaning that frequencies higher than the highest tolerable continuous operating frequency can be applied. Driving the valve at overfrequencies is possible only a short time due the limited heating.

3 Technical Design

3.1 Basic Construction of the Hammer Valve

The bistable actuator presented in Uusitalo (2009) is transformed into a bistable hammer actuator by making small changes in the geometry. For example, the hydraulic armature and the anchor are modified to work as the target part and the accelerating part. As shown later in the results, the made changes altogether enable a reduced total radius and thus a reduced volume of the valve while the hydraulic flow rates remain approximately the same.

The basic geometry of the actuator consists of two coils (a pushing one and a pulling one), a permanent magnet with radial magnetization, and the magnetic circuit with an accelerating part. The target part can either be a magnetic part attached to the hydraulic armature or the hydraulic armature itself. Because of the long movement of the accelerating part, the air gaps in the magnetic circuit will be long. Luckily, the viscous friction will be smaller for the same reason. Also, there is the flow path for the bypassing oil represented later in Fig. 4. The relation of the masses between the target part and the accelerating part is convenient for hammer actuating, since the accelerating part is heavier (1.9 g) than the target part (1 g). The geometry of the valve is presented in Fig. 1.

The hydraulic part used in this work, first presented in Lauttamus (2006), is a seat part that has pressure compensation when opened. The basic idea is to lead a pressure between the input and output pressures to the top of the armature to compensate the hydraulic forces. This "middle pressure" above the armature is gained using several restrictions in the seat, making drillings to the armature as seen in Fig. 1 and leading the pressure before the last restriction (the only sealing restriction at closed position) to the top.

A comparison of the opening forces between the designed hydraulic part and a traditional hydraulic part is presented in Fig. 2. The designed hydraulic part requires an opening distance of 0.6 mm and a force of 48 N at a 210 bar pressure difference over the valve.

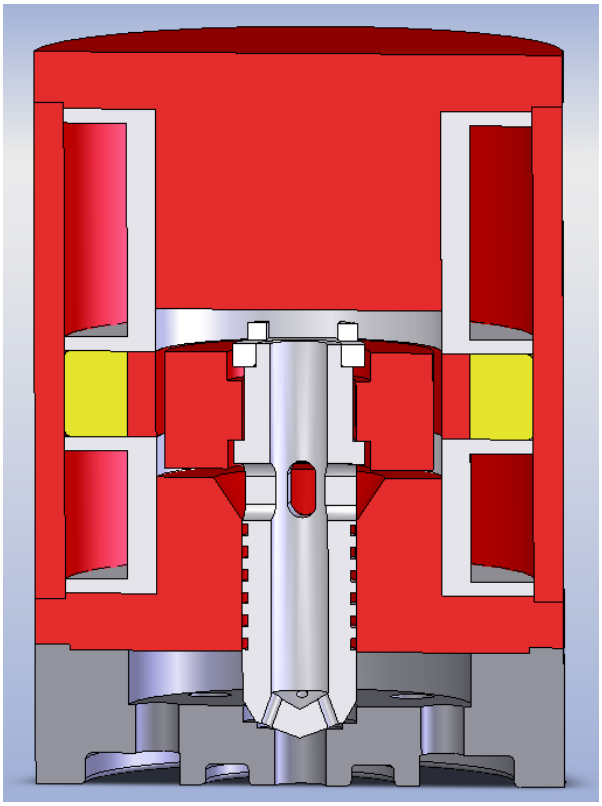

Fig. 1: *The geometry of the hammer valve. All red parts are made of armco iron and the yellow part is the permanent magnet ring. The height of the actuator structure is 22 mm and the total height of the valve is 26 mm. The diameter of the valve is 18.5 mm*

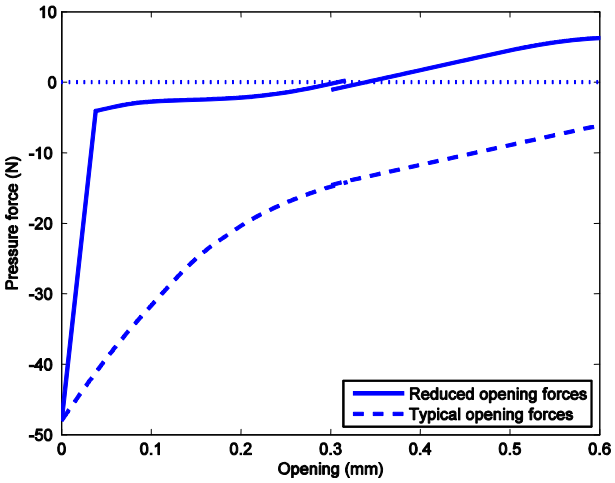

Fig. 2: *Pressure forces of a typical seat valve (typical opening forces) compared with a seat valve with several restrictions (reduced opening forces). The hydraulic part with reduced opening forces is presented in (Lauttamus, 2006)*

Structurally, the chosen bistable hammer actuator resembles the geometry of the bistable actuator presented in Burmeister (1967) and Fig. 3. Both solutions have a radially magnetized permanent magnet between two coils. However, the hammer actuator in this thesis differs from the previous actuator as follows:

- The hammer actuator was made thinner to pack several parallel valves in the small space of the valve package.
- In the hammer actuator, the coils are used simultaneously whereas Burmeister (1967) recommends use of one coil for each switching direction.
- The hammer actuator embodies hammer actuation.
- Considerable effort was put in multiphysically designing the hammer valve. For example, the oil flow around the anchor was modeled simultaneously with electromagnetic forces.

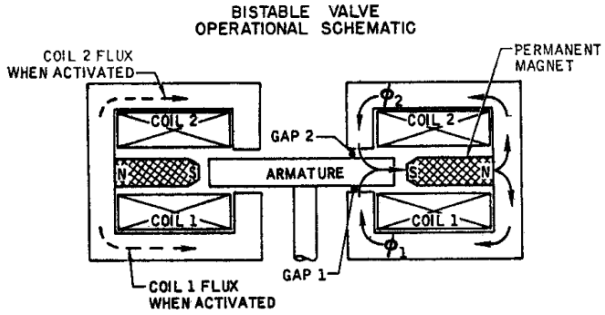

Fig. 3: *A bistable actuator in (Burmeister, 1967), page 146*

3.2 Operation Mode

Here is a detailed but intuitive description of the operation mode of the bistable hammer actuator. The electromagnetic behavior of the hammer actuator is similar to the bistable actuator presented in Uusitalo (2009). Therefore, the description of the electromagnetic behavior given here is not as exact as in the corresponding description found in Uusitalo (2009).

- Before opening, the permanent magnet holds the accelerating part in its lower position (closed valve).
- When the voltage of the coils is turned on, the current and thus magnetic flux start to rise and screening currents are induced. The flux of the permanent magnet is strengthened above the accelerating part and weakened below it (Fig. 6).
- When the electromagnetic force exerted on the accelerating part is positive (upwards) it starts to move up. At the same time viscous friction starts to repulse the movement. The viscous friction increases as the speed increases. On the other hand, viscous friction depends also on the position, but only slightly, if the collision phase is not considered.
- When the accelerating part is close to the target part (hydraulic armature) the viscous friction starts to increase quickly due to the squeeze effect (collision via a thin oil sheet between the two metal parts). A strong and sudden impulse force is exerted on both the target part and accelerating part. This squeeze effect is not modelled in this research. Collision modelling as described was used.
- If the impulse force is high enough, it overcomes the hydraulic pressure force and the target part starts to move together with the accelerating part.
- As the target part moves the hydraulic forces drop rapidly due to pressure compensation in the hydraulic part.
- During the collision process, the accelerating part is slowed down a lot, but if the initial speed before the collision is high enough, the movement and opening continues until the valve is fully opened. The movement is stopped when the target part hits the magnetic circuit.
- During the movement, the current of the coils changes. Before the collision, the current may decrease because of a current induced to the coils by the movement of the magnetic part, if the movement is fast enough. Also, the current may rise when the magnetic accelerating part is slowed down and decrease again when the accelerating part and target part accelerate again after the collision, if the accelerations are big enough.
- When the movement is over, the voltage is set off. After the screening currents and magnetization due to voltage pulse in the magnetic circuit have vanished, the permanent magnet holds the accelerating part and thus target part in the upper position. The target part is held in the upper position also by a hydraulic forces (if there is a pressure difference over the valve), because of the bistable form of the hydraulic force curve.
- Closing the valve works the same way. Only the hydraulic force needed to be exceeded by the impulse force is much lower.

4 Modelling

The exact modeling of the hammer actuator leads to a coupled modeling problem between dynamic nonlinear electromagnetic field, dynamic nonlinear fluid mechanical turbulent and/or laminar flow and mechanical movement calculations. However, it is impossible to take all these phenomena accurately into account in a numerical multiphysical modeling process. Therefore simplifications to the modeling process must be made while the accuracy of the calculations is still attempted to be kept at a good level. Modelling is made using different software tools, because no tools with accurate nonlinear electromagnetic time dependent motion coupled solver also equipped with fluid mechanical solver were known to the authors. The goodness of the models is determined by the measurements.

The geometry in the models differs a little from the actual prototype. The prototype is a 3D design but it is approximated with 2D axisymmetric models in all modeling cases. Furthermore, dynamics of the oil is not taken into account in the models. Also, the hysteresis in electromagnetic computations, mechanical friction and stiction effects (Resch, 2008) are ignored due to the challenges of their modelling compared to the benefits. However, the viscous friction forces are computed as explained in the next section.

4.1 Fluid Mechanical Modeling

Measured data from Lauttamus (2006) is used to model hydraulic pressure forces (later: hydraulic forces) exerted on the hydraulic armature (target part). Static models are used to calculate pressure forces due to viscous friction (later: viscous friction forces) at different locations and speeds. This data is used when the electromagnetic computation with movement modeling is carried out.

In static fluid mechanical modeling the general equations for incompressible flow are solved. In practice, solutions are found easily only when laminar flow occurs. That is typically, when the Reynolds number is under 2000. The flow bypassing the moving parts in the viscous friction calculations presented in this paper is almost always laminar. Only when the velocity of the moving parts exceeds about 2 m/s which corresponds in the used geometry the Reynolds number about 2000 or the accelerating part is very close to the target part, the bypassing flow changes from laminar to transient or turbulent flows. Turbulent flows are not modeled. Instead, when the laminar model cannot be solved anymore, in case of high speed movement (over 2 m/s) of the anchor that is, extrapolation from laminar models is used. In case of accelerating part being very close to target part, collision modeling in form of an artificial impulse force and extrapolation are used.

Figure 4 represents some of the calculated viscous friction data. In this case the anchor and hydraulic armature are moving towards opened position. It turns out, that the position of the moving parts does not affect greatly to the viscous friction force. On the other hand, the speed and number of moving parts do. This makes Fig. 4 a rather exact model of the viscous friction force in the opening case. The viscous friction force in closing phase was assumed to be similar to the opening phase, but with an opposite sign.

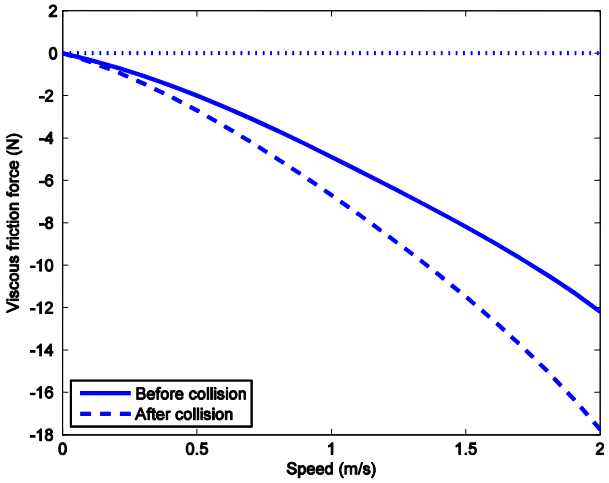

Fig. 4: *Viscous friction force before and after the collision the part(s) moving in opening direction*

Figure 5 represents the velocity and pressure field models of one calculated motion case for viscous friction force calculation. In the model, the accelerating part is moving up just before the collision. On all it's borders there is a boundary condition of an up going flow adjusted to the velocity of the accelerating part. The viscous force exerted on the accelerating part is calculated from the pressure field. The viscous friction force is calculated using several positions and velocities of the accelerating (and target) part(s). The fluid mechanical models were computed with Comsol multiphysics using a high number of elements. Computing time was not a problem since only static laminar cases were solved.

4.2 Electromagnetic Modeling

The linear motion model employed takes all the needed dynamical electromagnetic phenomena into account, including the movement (back-EMF effect), magnetic diffusion, eddy current and earlier pulses in cycling. The used OPERA-2d linear motion software solves the vector diffusion equation with the magnetic vector potential A as the unknown variable. In a 2D cylinder-symmetric case, A is simplified to $A_\phi\, u_\phi$, where u_ϕ is the unit vector in the angular direction. The full problem is thus given as follows (all in the angular direction):

Domain Ω: Find A_ϕ such that

$$-\frac{\partial}{\partial z}\left(\frac{1}{\mu}\frac{\partial A_\phi}{\partial z}\right)-\frac{\partial}{\partial r}\left(\frac{1}{\mu r}\frac{\partial\left(rA_\phi\right)}{\partial r}\right)-\sigma\left(\frac{\partial A_\phi}{\partial t}\right)= \frac{\partial H_{c,r}}{\partial z}-\frac{\partial H_{c,z}}{\partial r}+\sigma\frac{1}{r}\frac{\partial V}{\partial \phi} \quad (1)$$

holds for all x ∈ Ω and fulfils the given boundary conditions on the boundary ∂Ω.

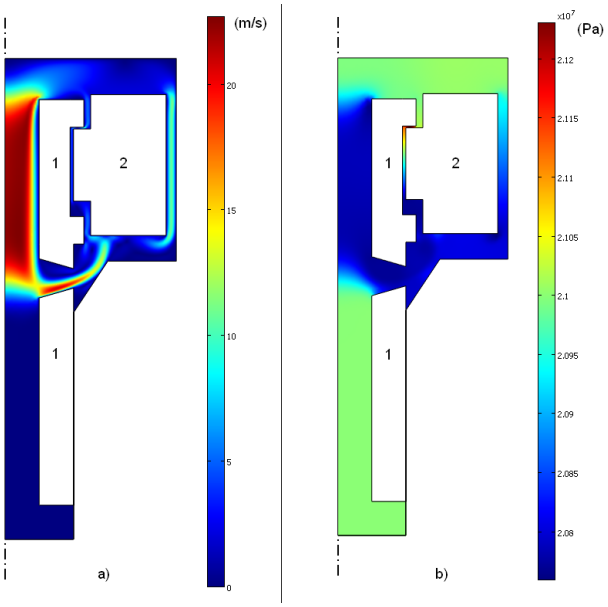

Fig. 5: *This figure represents typical velocity (a) and pressure (b) fields calculated with the fluid mechanical models. Parts: 1. the target part, hydraulic armature, 2. the accelerating part, anchor*

The current density in Eq. 1 has been split into driving source (voltage V driven model), $\sigma\frac{1}{r}\frac{\partial V}{\partial \phi}$, and induced currents, $-\sigma\left(\frac{\partial A_\phi}{\partial t}\right)$. The coercive force of the

permanent magnet H_c is now given as $H_{c,r}$ and $H_{c,z}$. The equations are given in the Lagrange coordinate system. The conductivity value σ of the used armco iron was set to 10^7 S/m in all models. After the magnetic vector potential has been numerically solved, forces can be evaluated, for example, integrating the so called Maxwell stress tensor (MST) over the anchor (Stratton, 1941). The used models are presented more elaborated for example in Uusitalo (2009).

Two typical magnetic field plots are given in Fig. 6. On the left the magnetic field before an opening pulse (valve closed). On the right a typical situation where the magnetic field has a certain skin depth when an opening pulse is applied. The non-magnetic target part (hydraulic armature) was not modeled, nor were the copper rings on the windings.

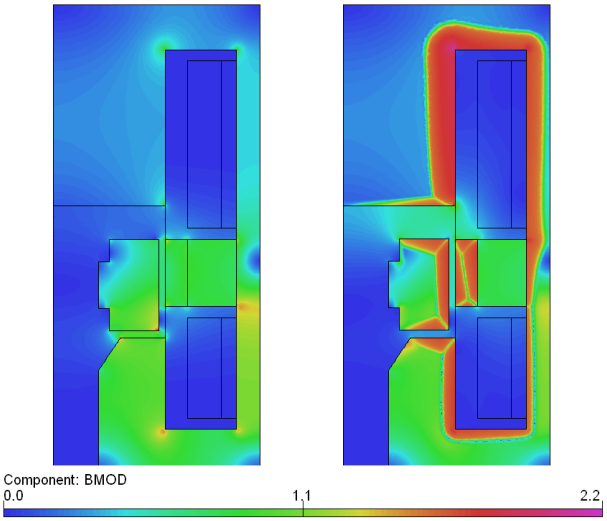

Fig. 6: *Magnetic fields plots (fields in Teslas)*

4.3 Mechanical Modeling

In the collision modeling it assumed that the oil is incompressible and the collision is thus inelastic. In an inelastic collision there is often a permanent change in geometry in at least one of the colliding parts. However, in this case the deformation is the movement of the oil between the two colliding objects.

In an inelastic collision linear momentum is conserved but kinetic energy is not. The situation is hard to model with viscous friction calculations, because of arising turbulent flows. This is why the loss of kinetic energy is taken into account by artificially slowing down the accelerating part in the models with a constant artificial impulse force during the last micrometers before the collision. The constant artificial impulse force F is calculated with the principle of virtual work $\Delta W \approx F\Delta s$, where the energy ΔW is the calculated loss of kinetic energy, and Δs is the small displacement. In practice, the range of influence for the artificial impulse force is set to the point when the accelerating and target parts are less than 0.05 mm apart from each other. This is because at smaller gaps the viscous friction force cannot anymore be calculated with laminar models as mentioned above.

If the impulse force in the collision process is higher than the hydraulic force exerted on the hydraulic armature (target part) the flow path will open. Still, after the valve is just opened (ajar), the accelerating and target parts together must have enough kinetic energy to overcome the rest of the hydraulic force. This is because the hydraulic force does not drop to zero instantly although it drops rapidly (Fig. 2).

The modeled artificial impulse force might be smaller than the hydraulic force needed to be exceeded (and it is in many cases). In this case, the valve should not open according to models, but the prototype might still work. This is because the actual impulse force is not constant and it forms a relatively sharp peak. The maximum value of the peak cannot be calculated with the presented models, but if it is higher than the hydraulic force, the hammer valve will work. For these reasons, the functioning of the hammer valve – that is, at least fractional opening – is assumed in models. The actual functioning of the valve remains to be verified by measuring the valve prototype.

The movement is calculated by solving the electromagnetic boundary value problem including the effects of linear motion. In practice, we take into account:

- The electromagnetic forces.
- The measured hydraulic pressure forces from Lauttamus (2006) (represented in Fig. 2).
- The viscous friction forces from static fluid mechanical calculations (Fig. 4).
- The artificial impulse force that simulates the loss of energy in an inelastic collision.
- The mass of the accelerating part and in addition the mass of the target part, where applicable.

The mechanical movement calculations are done together with the electromagnetic calculations with the VF opera 2d linear motion software.

5 Prototyping

Figure 7 presents a size comparison between the bistable hammer actuator, a 9 V battery and the bistable valve presented in Uusitalo (2009). The geometry of the hammer valve prototype is presented in Fig. 1.

Fig. 7: *Size comparison between the bistable hammer actuator on the left, a 9 V battery in the middle and the bistable valve presented in (Uusitalo, 2009) on the right*

The coils are wound with copper wire of diameter 0.25 mm. The total number of rounds is 234 (146 in upper and 88 in lower coil). The computational total resistance of the two coils at 20 ºC is 3.8 Ω and 4.8 Ω at 80 ºC. Corresponding measured resistances are 3.6 Ω

at 22 ºC, 3.8 Ω at 32.3 ºC and 4.5 Ω at 80 ºC.

The type of the permanent magnet is ND-31SHR and the direction of its magnetization is radial (unipole). The winding did not fill all the space in the coil formers. The rest was filled with copper rings and silicon paste in order to improve thermal conductivity properties. Press fit was used to build the target part (hydraulic armature) from two separate parts. A solid pressure vessel in the hammer valve was left out. It is replaced with separate parts of the magnetic circuits and coil formers glued together.

6 Results

6.1 Modeled Behavior of the Hammer Valve

The valve has been planned to be operated with short 24 V voltage pulses. At this voltage level, the modeled response time at opening is 1.94 ms and 1.78 ms at closing. Figures 8 and 9 describe rms power consumption at 62.5 Hz drive and velocity of the accelerating part in case of various voltage pulse levels. All models are done at 80 ºC temperature and with a 210 bar pressure difference (Δp = 210 bar) at closed state.

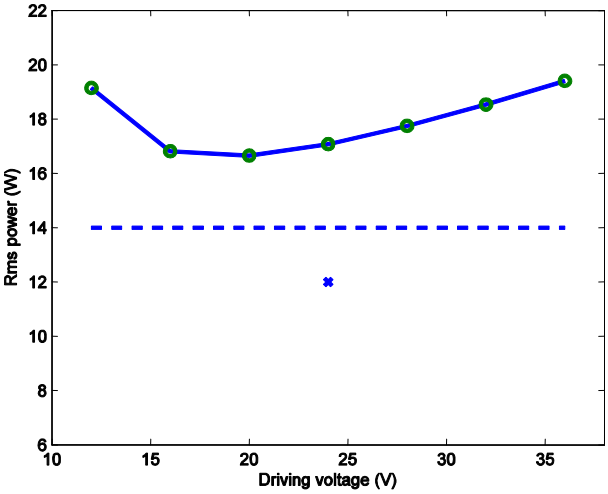

Fig. 8: *Modeled power consumption of the valve during the first cycle of a cycled 62.5 Hz drive. The dashed line shows the approximated maximum of continuously applicable rms power. The cross shows a case where the length of voltage pulses is reduced*

From Fig. 8 it can be seen, that a minimum in the rms power consumption curve can be found. Also, the approximated continuously applicable rms power seems to be lower than the power consuming of the valve at 62.5 Hz – no matter which voltage pulse level is chosen – unless shortened pulses are used. In this case the voltage pulse is kept on only until the collision takes place. The effect of the shortened pulse to the response time is less than 0.1 ms.

Rapid cycled driving of the hammer valve has similar effect to response times as in the bistable valve presented in Uusitalo (2009). That is, the response time of the second switch is bigger than in a single pulse. The response times in later cycles are only slightly bigger than in a single pulse. Also, a steady level of response times is reached after just a few cycles.

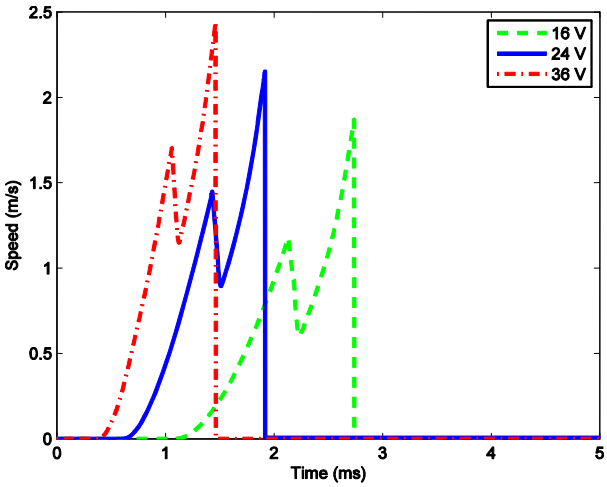

Fig. 9: *Velocity of the accelerating part with various voltage pulses according to models*

The modeled switching energies for the hammer valve are about 0.14 J for opening and 0.13 J for closing. For comparison, the bistable valve presented in Uusitalo (2009) needed about 0.68 J energy from the voltage source for the opening switch.

In the modeling cases, when a hydraulic input pressure of 210 bar is used, the output pressure is assumed to be close to 1 bar when the valve is closed and 110 bar (Δp = 100 bar) when the valve is opened.

6.2 Measured Results and Comparison to Models

The measurement setup was a hydraulic circuit that consisted of a hydraulic pump system, the hammer valve, pressure sensors, a flow sensor and a thermal sensor. Hydraulic diagram of the test circuit is shown in the Fig. 10. The valve was powered by a voltage pulse source. There was also a heater which was used to gain a high and steady 80 ºC operation temperature for the valve.

First, the functioning of the hammer valve was verified. The pressure difference was set to 210 bar and the valve was heated to 80 ºC. The valve worked with 18 V driving voltage with 10 ms voltage pulses. At 24 V driving voltage the valve worked approximately according to the models, with a response time (measured from pressure) and voltage pulses of slightly under 2 ms.

Comparison of measured and modeled currents of a 24 V 62.5 Hz drive is presented in Fig. 11. The modeled rms power consuming is 17.1 W and the measured 17.0 W. The voltage pulses in the measured case were slightly shorter. The limit of 14 W would computationally be achieved with a continuous operating frequency of about 51.5 Hz. The back-EMF effect is visible in both modeled and measured current curves.

The functioning of the valve at high operating frequency is presented in Fig. 12. It can be seen that some pressure oscillation occurs as the pressure difference reaches values higher than the input pressure of 210 bars. For this reason, it is hard to approximate the response times very accurately.

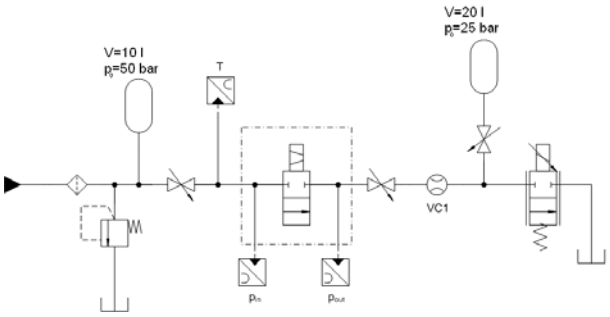

Fig. 10: *Hydraulic diagram of the test circuit*

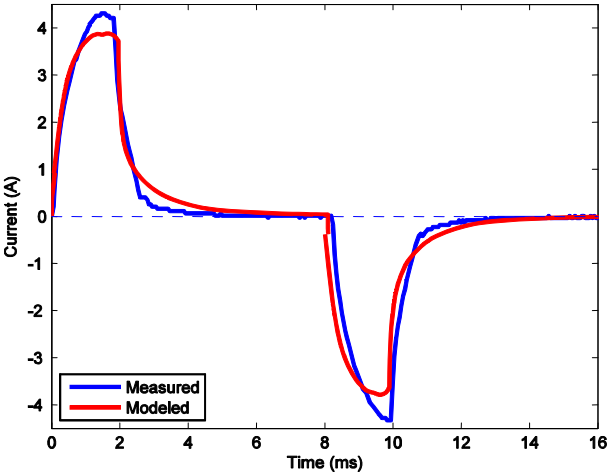

Fig. 11: *Comparison of measured and modeled currents. Operating frequency was 62.5 Hz and driving voltage was 24 V*

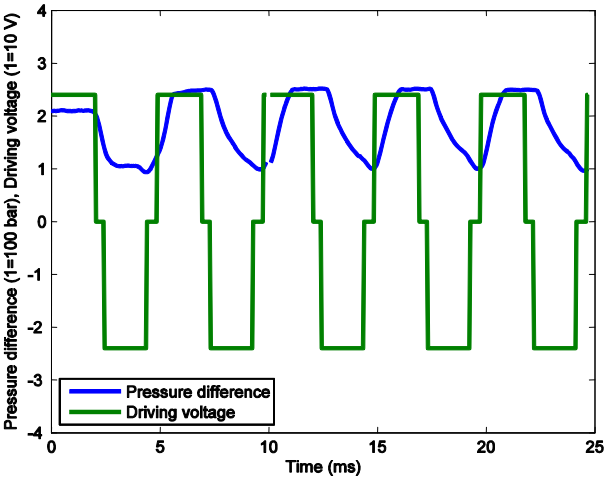

Fig. 12: *Pressure difference and driving voltage at 200 Hz cycled drive*

The measured response times were set to the time gap between starting the voltage to the first noticeable change in pressure. This is also the end of the voltage pulse. In cycling, the length of the voltage pulse is remained the same in later pulses even thought the pressure change does not anymore correspond to the pulse time. From Fig. 12 it can be seen, that the valve opens and closes each time nevertheless.

The pressure difference – flow rate curve (pQ-curve) of the hammer valve is presented Fig. 13. The flow rate curve is significantly changed from earlier similar design presented in Uusitalo (2009) and Lauttamus (2006). These changes are due to changed geometries in the flow channels. The cavitation effects are now smaller and the maximum flow is relatively high, but the downside is that the flow curve is now flatter.

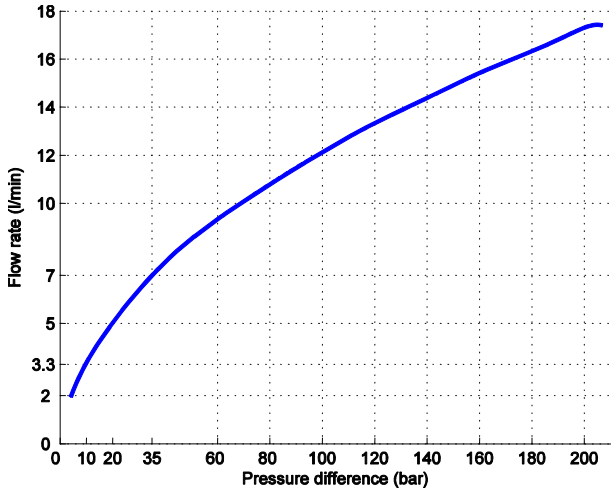

Fig. 13: *Pressure difference – flow rate curve with supply pressure of 210 bar. The temperature of the oil was about 30 ºC*

The used electronics causes an overshoot of about 5 % in the applied voltage in the measurements. All presented measurements were done with about 30 ºC oil temperature and 80 ºC valve temperature.

As last study case, the response times were measured with various pressure differences. The result was that the pressure difference (any given Δp between 0 bar and 210 bar when valve closed) does not affect the response time noticeably. After this, the valve was subjugated to rather heavy cycling of about 30000 rounds. Then, the response times were measured again. The result was that the response times had increased 10 - 20 %, at least at higher flow rates.

In Uusitalo (2010) several copies of the hammer valve were made in order to build a digital hydraulic valve package. According to the measurements on different copies and modifications, the number of applied cycles could be increased from 30000 to 500000 (we stopped there) by hardening the hydraulic parts. However, the made modifications also increased the response time.

6.3 Comments on the Measurements

In measured results, the prototypes response times are measured from pressure changes. The pressure change is sensed with a pressure sensor that has a delay about 0.4 ms. On the other hand, the modeled response times are set to the time gap between giving the voltage pulse until the end of the anchor movement (also end of the voltage pulse). If the anchor moves at an average speed of 1.5 m/s it takes about 0.4 ms to travel the 0.6 mm opening distance for it. For these reasons, the measured and modeled response times should still be, and they are, reasonably close to each other. Anchor position measuring would be a better way to measure the response time from the prototype. The problem in this however, is the high pressure of the oil inside the valve.

The hydraulic part of the hammer valve worked almost the same as in the bistable valve presented in Uusitalo (2009) and Lauttamus (2006), although the nominal flow rates were slightly reduced. The valve jammed a few times during running-in, but later the jamming disappeared. The jamming was probably due to some small inaccuracy in prototype construction, for example roughness of the sliding surfaces. The wearing and tearing of the hydraulic part found in the bistable valve presented in Uusitalo (2009), was confirmed again after heavy cycling. As shown in Uusitalo (2010), this can be prevented by using some hardening methods for the hydraulic parts.

The problems in the hydraulic part do not concern the hammer actuator, which works almost as modeled. This means, that the assumptions in multiphysic modeling were reasonable. The neglecting of mechanical frictions probably causes most of the difference between the models and measurements. There might also still be some stiction forces. Other remarks on the prototype are that the pressure vessel was leak-proof and the valve functioning at lower temperatures (30 ºC) was also verified by measurements.

The radially magnetized permanent magnet ring of the hammer actuator seems to be a good choice for three reasons. First, the permanent magnet is not easily demagnetized because it is not exposed to collisions. Second, the permanent magnet is almost only strengthened by voltage pulses, which further decreases the risk of demagnetization. The third reason is that the volume of the valve seems to be minimized when the magnet is placed between the coils (Fig. 1).

The approximated highest tolerable rms power (14 W) of the hammer valve presented in Fig. 8 was measured when the valve was placed to its manifold (and the manifold was attached to some metal structures). When the valve is placed alone on the table the maximum applicable rms power rate drops from 14 W to about one tenth. This is because the valve can emit more heat when placed to its manifold with a larger surface area. This should be noted when designing a valve package. However, the cooling effect of the bypassing oil was not taken into account. Furthermore, the rms power rate of a single hammer valve could maybe be reduced to about 12.0 W by using shorter pulses as shown in models. The change in response time is less than 0.1 ms, but this was not confirmed with measurements.

6.4 Comparison to Commercial Valves

A hammer valve construction was successfully established. Comparison between several seat valves – Flocontrol valve (Linjama, 2005), Lee valve (number SDBB3322013A) (Lee, 2005), Hydac WS08W-01, bistable valve presented in Uusitalo (2009) and the hammer valve – is presented in Table 1. There is also one spool valve, Moog NG6, for comparison. The information on Moog and Hydac valves are based on measurements on individual valves at the Department of Intelligent Hydraulics and Automation. The Hydac valve is a seat valve with a dynamic seal.

In Table 1, the switching times have all been measured without any booster circuits and the operating frequency means the maximum continuous operating frequency. For the volume of the valve only the volumes of electromagnetic actuator and active hydraulic parts are considered (excluding all pipes and terminals). We define the nominal flow density q_{nom} as (Nominal flow rate/Volume). Some of the valves will not work at a 210 bar pressure difference without an extra restriction in series with the valve. For these valves, maximum flow rates and maximum flow densities (which we define as q_{max} = (Theoretical maximum flow/ Volume) are calculated in order to find out the maximal level of performance for each valve.

Table 1: Comparison of the hammer valve, the bistable valve presented in (Uusitalo, 2009) and some in-market valves. Properties of valves: 1. Response time t (ms), 2. Maximum continuous operating frequency f_{con} (Hz), 3. Maximum operating frequency f_{max} (Hz), 4. Nominal flow rate Q_{nom} (l/min) @ Δp = 10 bar, 5. Maximum flow Q_{max} (l/min), 6. Maximum pressure differential Δp_{max} (bar), 7. Volume *Volume* (cm³), 8. Nominal flow density q_{nom} ((l/min)/cm³) @ Δp = 10 bar, 9. Maximum flow density q_{max} ((l/min)/cm³) @ Δp = 210 bar

Property	Hammer valve	Bistable valve	Flo-control	Lee valve	Moog NG6	Hydac
1. t (ms)	**~ 2**	< 3.5	7-15	< 30	> 20	> 20
2. f_{con} (Hz)	**> 50**	~ 30	?	20	5	?
3. f_{max} (Hz)	**200**	100	?	20	5	?
4. Q_{nom} (l/min)	3.3	4.4	0.8	0.5	100	17
5. Q_{max} (l/min)	17	18	3.7	?	212	34
6. Δp_{max} (bar)	210	210	210	?	45	40
7. *Volume* (cm³)	7.0	21.3	~ 58	~18.5	~ 400	~ 80
8. q_{nom} ((l/min)/cm³)	**0.47**	0.21	0.014	0.027	0.25	0.21
9. q_{max} ((l/min)/cm³)	**2.4**	0.94	0.064	?	0.53	0.43

For comparison with the valves presented in Table 1, it is mentioned that there exist also another fast spool valve – the Sturman valve (Johnson, 2001) This valve has the following characteristics: response time is 0.45 ms, flow at Δp = 10 bar is 17.3 l/min, volume is about 40 cm³ and thus its calculated nominal flow density (at Δp = 10 bar) is 0.43 ((l/min)/cm³). The maximum pressure difference and operating frequencies of the Sturman valve are unknown to the author. Also, the Sturman valve is not fully comparable with the valves presented in Table 1, because it uses electronic boosting. That is, the Sturman valve is current controlled instead of traditional voltage control. As mentioned above, boosting would also probably benefit the valves presented in Table 1, but this factor was left out of the study.

7 Summary

It is concluded that the designed bistable hammer valve meets the needs of digital hydraulics as it is small and fast with a high operating frequency. Furthermore, the response time of the valve is almost pressure difference independent, which is a useful property for a valve in a digital hydraulic control system, since the response time can be well predicted. The hammer valve also has a high flow density number in comparison to commercial valves. For these reasons the novel hammer valve is found competitive.

Nomenclature

A	Magnetic vector potential	$\frac{Wb}{m}$
A_ϕ	Angular component of magnetic vector potential	$\frac{Wb}{m}$
F	Force	N
f_{con}	Continuous operating frequency	Hz
f_{max}	Maximum (transient) operating frequency	Hz
H_c	Coercive force of the permanent magnet	$\frac{A}{m}$
$H_{c,r}$	Radial component of the coercive force	$\frac{A}{m}$
$H_{c,z}$	Axial component of the coercive force	$\frac{A}{m}$
q_{nom}	Nominal flow density	$\frac{\frac{l}{\min}}{cm^3}$
q_{max}	Maximum flow density	$\frac{\frac{l}{\min}}{cm^3}$
Q_{nom}	Nominal flow	$\frac{l}{\min}$
Q_{max}	Maximum flow	$\frac{l}{\min}$
t	Response time	s
u_ϕ	Unit angular vector	
V	Voltage	V
Δp	Pressure difference	bar = 10^5 Pa
Δp_{max}	Maximum pressure difference	bar = 10^5 Pa
Δs	Small displacement	m
ΔW	Virtual work	J
μ	Permeability	$\frac{N}{A^2}$
σ	Conductivity	$\frac{1}{\Omega \mathrm{m}}$

References

Burmeister, L., **Loser, J.** and **Sneegas**. 1967. *E. NASA Contributions to Advanced Valve Technology, 2nd edition.* Office of Technology Utilization, NASA, Washington D.C, USA.

Garstenauer, M. and **Scheidl, R.** 1999. High-speed switching valves actuated by parametrically excited structures. *Power Transmission and Motion Control, PTMC'99*, pp. 137 - 150, Bath, UK.

Johnson, B., **Massey, S.** and **Sturman**. 2001. O. Sturman digital latching valve. In J.-O. Palmberg, editor. *Proc. of The Seventh Scandinavian International Conference on Fluid Power*, SICFP'01, volume 3, pp. 299 - 314, Linkoping University, Linkoping, Sweden.

Kajima, T. and **Kawamura, Y.** 1995. Development of a high-speed solenoid valve: Investigation of solenoids. *IEEE Transactions on industrial electronics*, 42(1), pp. 1387 - 1390.

Kallenbach, E., **Kube, H.**, **Zoeppig, V.**, **Feindt, K.**, **Hermann R.** and **Beyer, F.** 1999. New polarized electromagnetic actuators as integrated mechatronic components – design and application. *Mechatronics*, 9(7), pp. 769 - 784.

Karvonen, M., **Uusitalo, J. P.**, **Ahola, V.**, **Linjama**, **M.** and **Vilenius, M.**. 2009. A novel symmetric and bistable seat valve. *The 11th Scandinavian International Conference on Fluid Power, SICFP'09*. Linkoeping, Sweden.

Lauttamus, T., **Linjama, M.**, **Nurmia, M.** and **Vilenius, M**. 2006. A novel seat valve with reduced axial forces. *Bath Workshop on Power Transmis-*

sion and Motion Control, PTMC'06, pp. 426 - 438, Bath, UK.

The Lee Company. 2003. *Technical Hydraulic Handbook*, Release.

Lesquesne, B. 1990. Fast acting, long-stroke solenoids with two springs. *IEEE Trans. Indust. Appl., 26*, pp. 845 - 856.

Linjama, M. and **Karvonen, M.** 2003. Digital microhydraulics. *The First Workshop on Digital Fluid Power, DFP'08*, pp. 141 - 152. Tampere, Finland.

Linjama, M., **Tamminen, P.**, **Andersson, B.** and **Vilenius, M.** 2005. Performance of the valvistor with digital hydraulic pilot control. *The Ninth Scandinavian International Conference on Fluid Power, SICFP'05*, pp. 14 on CD–ROM, Linkoping, Sweden.

Linjama, M. and **Vilenius, M.** 2007. Digital hydraulics – towards perfect valve technology. *The Tenth Scandinavian International Conference on Fluid Power, SICFP'07*, Vol. 1, pp. 181 - 196, Tampere, Finland.

Linjama, M. 2008. Digital hydraulics research at IHA. *The First Workshop on Digital Fluid Power, DFP'08*, pp. 7 - 30. Tampere, Finland.

Resch, M. and **Scheidl, R.** 2008. Oil stiction in hydraulic valves – an experimental investigation. *Fluid Power and Motion Control 2008*, Bath, UK.

Stratton, J. 1941. *Electromagnetic theory*, Vol. 2, McGraw-Hill.

Tsay, J., **Chang, H-A.** and **Sung, C-K.** Design and experiments of fully compliant bistable micromechanisms. Elsevier, *Mechanism and Machine Theory, 40*, pp. 17 - 31.

Uusitalo, J. - P., **Söderlund, L.**, **Kettunen, L.**, **Linjama, M.** and **Vilenius, M**. 2009. Dynamic analysis of a bistable actuator for digital hydraulics. *IET Science, Measurement & Technology, 3(3)*, pp. 235 - 243.

Uusitalo, J. - P. 2010, *A Novel Digital Hydraulic Valve Package: A Fast and Small Multiphysics Design.* PhD thesis, Tampere University of Technology, Tampere, Finland.

Jukka-Pekka Uusitalo
was born in 1980 in Hyvinkää, Finland. He graduated as MSc in 2006 and PhD in September 2010 from Tampere University of Technology. His PhD concerned digital hydraulics, especially digital valves. He is currently working as a researcher at Electromagnetics, Tampere University of Technology.

Ville Ahola
was born in Lappajärvi, Finland on May 28 1981. He graduated as MSc in May 2008 from Tampere University of Technology. He is currently working as a researcher/PhD student in the department of Intelligent Hydraulics and Automation at Tampere University of Technology.

Lasse Söderlund
was born in 1960 in Turku, Finland. He graduated as MSc in 1984 and as Lic. Eng. in 1999 from Tampere University of Technology. He is currently working as a laboratory engineer at Electromagnetics, Tampere University of Technology.

Matti Linjama
(Born 4th July 1971) is Adjunct professor and works at the Department of Intelligent Hydraulics and Automation (IHA), Tampere University of Technology (TUT), Finland. He graduated as Dr. Tech in 1998 from Tampere University of Technology. Currently he is leader of digital hydraulics research group in IHA.

Maarit Juhola
was born in 1979 in Alastaro, Finland. She graduated as MSc in 2009 from Tampere University of Technology and she has been a PhD student since that year. Her research concerns digital hydraulics, especially digital valves. She is currently working at Electromagnetics, Tampere University of Technology.

Lauri Kettunen
was born in 1962 in Espoo, Finland. He graduated as MSc in 1987 and as PhD in 1992 from Tampere University of Technology. He is currently working at Tampere University of Technology as a professor of Electromagnetics.